Anal. Chem. **2007,** *79,* 4493−4498

Sputtering Yields for C_{60} and Au_3 Bombardment of Water Ice as a Function of Incident Kinetic Energy

Michael F. Russo, Jr., Christopher Szakal, Joseph Kozole, Nicholas Winograd, and Barbara J. Garrison*

Department of Chemistry, Penn State University, 104 Chemistry Building, University Park, Pennsylvania 16802

The total sputtering yields for water ice due to kiloelectronvolt cluster bombardment have been measured and compared to the predictions made by the mesoscale energy deposition footprint (MEDF) model. For C_{60} bombardment, the experimental yield varies almost linearly from 820 water molecule equivalents at an incident kinetic energy of 10 keV to 10 100 water molecule equivalents at a kinetic energy of 120 keV. For Au_3 bombardment, the experimental yield varies almost linearly from 630 water molecule equivalents at an incident energy of 10 keV and rises to 1200 water molecule equivalents at 25 keV. The MEDF model is used to calculate relative yield trends with respect to incident energy using short-time molecular dynamics simulations. The results of these calculations indicate that the model can effectively predict the yield trends observed for these two clusters in experiments, although there is a consistent overestimate of the predicted induced C_{60} yield. It is hypothesized that this overestimate can be explained by the absence of reactions and ionization processes in the current simulations. Despite this omission, experimental yield trends can be accurately predicted using relatively small amounts of computer time. The success of the model in predicting the yield of water from ice films using a variety of energies and projectiles suggests this approach may greatly aid in the optimization of experimental configurations.

The use of polyatomic projectiles in secondary ion mass spectrometry (SIMS) has greatly expanded applications in imaging and depth profiling of molecular substrates. There are presently two types of projectiles under intense development: those based upon liquid metal ion gun (LMIG) technology (Au_3 and Bi_3)[1,2] and those that contain a larger number of atoms (SF_5, C_{60}, and Au_{400}).[3−7] The LMIG technology is appealing since the probe size can be easily reduced to a submicrometer size and is well-suited for imaging. The larger clusters deposit their energy near the surface resulting in improved sputtering yields and less subsurface chemical damage;[8−10] however, they are more difficult to focus. The observation that there can be reduced subsurface damage has created the vision that molecular depth profiling accompanied by lateral imaging might be possible.[10−13] The objective, thus, is to design the beam characteristics so that there is low substrate damage, high yield, and good focusing ability.

Molecular depth profiling with minimal accompanying chemical damage occurs when the molecular sputtering yield is high and the damage depth is low. To obtain larger yields, both molecular dynamics simulations[9,14] and experiment[15] suggest that, when the kinetic energy of the projectile is increased, the sputtering yield increases. Additionally, an increased kinetic energy results in better focusing ability.[10,15] Thus, a promising strategy is to increase the incident energy of the ion beam. Presently, the kinetic energies associated with commercially available ion sources are in the range of 5−25 keV for Au_3 and Bi_3 and 5−40 keV for C_{60}.[1,15] In some cases, multiply charged ions may be produced, increasing the kinetic energy of C_{60}^{3+} to 120 keV.[15]

The total yield of ejected material can be measured for various incident energies of the ion beam, but it is not possible to make a direct measurement of the energy deposition profile within the substrate, a necessary quantity in order to estimate damage and implantation of the beam. Computer simulations have been the method of choice to help guide the optimization of these parameters. Computer modeling in this kinetic energy range is problematic however, since the size of the substrate must be increased to a very large number of atoms in order to contain the important energy dissipation processes. The calculation of a single

* To whom correspondence should be addressed. E-mail: bjg@psu.edu.

(1) Davies, N.; Weibel, D. E.; Blenkinsopp, P.; Lockyer, N.; Hill, R.; Vickerman, J. C. *Appl. Surf. Sci.* **2003**, *203*, 223−227.
(2) Touboul, D.; Kollmer, F.; Niehuis, E.; Brunelle, A.; Laprevote, O. *J. Am. Soc. Mass Spectrom.* **2005**, *16*, 1608−1618.
(3) Appelhans, A. D.; Delmore, J. E. *Anal. Chem.* **1989**, *61*, 1087−1093.
(4) Blain, M. G.; Dellanegra, S.; Joret, H.; Lebeyec, Y.; Schweikert, E. A. *Phys. Rev. Lett.* **1989**, *63*, 1625−1628.
(5) Gillen, G.; King, R. L.; Chmara, F. *J. Vac. Sci. Technol., A* **1999**, *17*, 845−852.
(6) Wong, S. C. C.; Hill, R.; Blenkinsopp, P.; Lockyer, N. P.; Weibel, D. E.; Vickerman, J. C. *Appl. Surf. Sci.* **2003**, *203*, 219−222.
(7) Tempez, A.; Schultz, J. A.; Della-Negra, S.; Depauw, J.; Jacquet, D.; Novikov, A.; Lebeyec, Y.; Pautrat, M.; Caroff, M.; Ugarov, M.; Bensaoula, H.; Gonin, M.; Fuhrer, K.; Woods, A. *Rapid Commun. Mass Spectrom.* **2004**, *18*, 371−376.
(8) Castner, D. G. *Nature* **2003**, *422*, 129−130.
(9) Postawa, Z.; Czerwinski, B.; Szewczyk, M.; Smiley, E. J.; Winograd, N.; Garrison, B. J. *Anal. Chem.* **2003**, *75*, 4402−4407.
(10) Winograd, N. *Anal. Chem.* **2005**, *77*, 142A−149A.
(11) *Appl. Surf. Sci.* **2006**, *252*, 6403−7326.
(12) Cheng, J.; Wucher, A.; Winograd, N. *J. Phys. Chem. B* **2006**, *110*, 8329−8336.
(13) Cheng, J.; Kozole, J.; Hengstebeck, R.; Winograd, N. *J. Am. Soc. Mass Spectrom.* **2007**, *18* (3), 406−412.
(14) Anders, C.; Urbassek, H. M. *Phys. Rev. B* **2004**, *70*, 155404.
(15) Fletcher, J. S.; Conlan, X. A.; Jones, E. A.; Biddulph, G.; Lockyer, N. P.; Vickerman, J. C. *Anal. Chem.* **2006**, *78*, 1827−1831.

10.1021/ac070105l CCC: $37.00 © 2007 American Chemical Society
Published on Web 05/16/2007

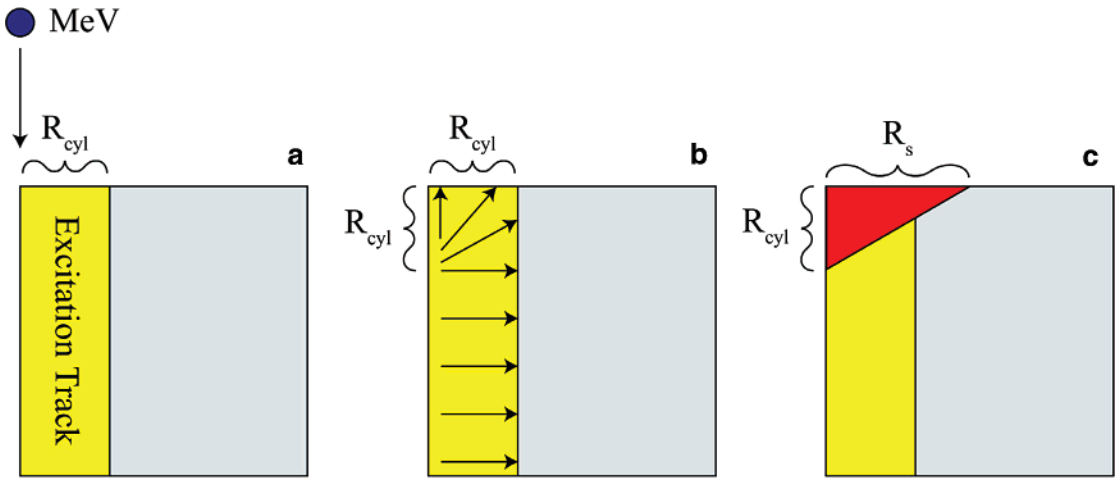

Figure 1. Schematic of the fluid dynamics track model. There is an implied cylindrical symmetry around the left edge of the figures. (a) Incident MeV particle and excitation track of radius R_{cyl}. (b) Arrows showing the general initial direction of motion of the particles. (c) Schematic showing conical volume of ejected material (in red).

trajectory may require several months or years of computer time under these conditions. Because of this difficulty, very little is known about the details of the energy dissipation of cluster projectiles in this kinetic energy range, particularly for molecular substrates.

In this work, quantitative experimental measurements and theoretical calculations of the total sputtering yield from water ice for C_{60} bombardment with kinetic energies from 10 to 120 keV and for Au_3 bombardment from 10 to 25 keV were performed. The experimental measurements are performed using a quartz crystal microbalance protocol, which has been described in a previous publication.[16,17] The theoretical calculations are performed using a combination of short-time molecular dynamics computer simulations and the mesoscale energy deposition footprint (MEDF) model developed recently.[18] This model, which is based upon fluid dynamics calculations performed by Jakaset al.,[19] provides a means to estimate the yield of a system with only 250 fs of simulation time. In a recent paper, we outlined the details of this model and illustrated how it could be used to describe the yield differences and spatial extent of the original positions of the molecules between 5-keV C_{60} and Au_3 on amorphous water ice.[18] The results presented here indicate that while the yield produced with Au_3 is consistently lower when compared to that of C_{60}, there is a near-linear yield increase with increasing energy for both projectiles. Using the MEDF model, these trends can be effectively reproduced, allowing vital information to be obtained from short-time simulations and potentially allowing for more complex systems and potentials to be feasible.

METHODS

Experimental Information. The strategy for experimentally measuring the amount of removed water molecule equivalents for each energetic projectile impact has been previously described.[16,17] Briefly, water ice films 100−150 nm in thickness were prepared by controllably depositing 2×10^{-6} Torr water ice vapor (Varian Variable Leak Valve, Varian Inc.) onto a silver-coated quartz crystal microbalance (Maxtech TM-400, Maxtech Inc.) cryogenically cooled to 100 K. The resulting amorphous ice films were investigated by mass spectrometric-molecular depth profile analysis. Specifically, the molecular depth profiles were achieved using an incident projectile to etch through the ice films at specified time intervals and SIMS to characterize the eroded ice surface subsequent to the following sputter cycle. The primary ion species employed in this research include 10-, 15-, 20-, and 25-keV Au_3 ions[1] and 10-, 15-, 20-, 40-, 80-, and 120-keV C_{60} ions (Ionoptika, Ltd.).[6] The two highest C_{60} ion energies are achieved by using a Wien filter to select C_{60}^{2+} and C_{60}^{3+} ions with a 40-keV extraction voltage.[15] The ion sources are mounted at a 40° angle of incidence to a conventional time-of-flight-SIMS analyzer (BioTOF, Kore Inc.) equipped with cryogenic cooling capabilities.[20]

Computational Information. The MEDF model[18] was developed from the work of Jakas et al.[19] in which the ejection of substrate material due to a megaelectronvolt particle bombardment originates from an energetically excited region whose behavior is described using fluid dynamics. The excitation region is illustrated as a track (Figure 1a) along the path of the projectile with radius R_{cyl}, within which the substrate material is quickly displaced and energized. Due to this rapid expansion, material that is less than or equal to a depth of R_{cyl} from the surface is able to travel in the direction of the vacuum above the surface and escape (Figure 1b). Any material that is below a depth of R_{cyl} cannot escape due to collisions with other bulk atoms and expands radially.

After the initial impact and subsequent excitation, further ejection is possible.[19] As the excitation diffuses outward and material within the track is ejected, the boundary of both the energized track, and the surface, begins to blur. Material that was in the near-surface region, but became energized after some time, now has a chance to escape. This diffusion of heat leads to a second radius, R_s, from which additional material can be removed.

(16) Szakal, C.; Kozole, J.; Russo, M. F., Jr.; Garrison, B. J.; Winograd, N. *Phys. Rev. Lett.* **2006**, *96*, 216104.
(17) Szakal, C.; Kozole, J.; Winograd, N. *Appl. Surf. Sci.* **2006**, *252*, 6526−6528.
(18) Russo, M. F., Jr.; Garrison, B. J. *Anal. Chem.* **2006**, *78*, 7206−7210.
(19) Jakas, M. M.; Bringa, E. M.; Johnson, R. E. *Phys. Rev. B* **2002**, *65*, 165425.
(20) Braun, R. M.; Blenkinsopp, P.; Mullock, S. J.; Corlett, C.; Willey, K. F.; Vickerman, J. C.; Winograd, N. *Rapid Commun. Mass Spectrom.* **1998**, *12*, 1246-+.

The value of R_s is connected to R_{cyl} by the relation $R_s = \tilde{E}^{1/2}R_{cyl}$, where $\tilde{E}$ is the average excitation energy within the track relative to the cohesive binding energy of the substrate material, $\tilde{E} = (E_{exc}/U_0)$. By combining these concepts, any ejected material will originate from a conical region R_{cyl} deep and R_s wide (Figure 1c), thus making the yield, Y, equal to the volume of this cone multiplied by the number density, η_0, of the substrate, $Y = \eta_0(\pi/3)R_s^2R_{cyl}$. Inserting the relation given above for R_s gives $Y = \eta_0(\pi/3)R_{cyl}^3\tilde{E}$. From this expression for the yield, it is evident that only the average excitation and radius of the excitation track are needed to make an estimate for the yield of a particular event.

The fluid model is not sufficient to predict sputtering yields by itself since the values of R_{cyl} and $\tilde{E}$ cannot be determined. These values may be estimated, however, from molecular dynamics computer simulations performed during the first 250 fs of the bombardment event. These values are then used in the fluid dynamics expressions to estimate the yield and lateral extent, R_s, of the ejection volume. The procedure that was developed for mapping short-time MD information onto the fluid dynamics results consists of choosing a time when 90% of the initial KE of the cluster has been transferred to the substrate. For that time, a contour plot of the deposited energy profile is created. From the energy profile, R_{cyl} is determined and from the cylinder volume the average excitation energy $\tilde{E}$ is calculated.

The details pertaining to the molecular dynamics scheme including the potentials, substrate characteristics, and special constraints/considerations used for these simulations have been described elsewhere.[18] In this work, an amorphous water ice substrate was bombarded by either C_{60} or Au_3 at 5, 10, 15, 20, and 40 keV of incident energy normal to the surface. An additional trajectory for 80-keV C_{60} was also completed. The procedure was unsuccessful for 80-keV Au_3 bombardment since the Au atoms left the bottom of the sample before 90% of the energy was transferred. Each of these systems was monitored until the 90% energy transfer point was reached, requiring ~180 fs for C_{60} and ~300 fs for Au_3.. The crystal samples are not large enough to model the entire ejection event, and it is presently not feasible to increase their size further. For reference, the computer time required for the initial 5-keV simulations was ~4 months for each cluster.[21]

RESULTS AND DISCUSSION

The measured total sputtering yields for the two primary ion beams are presented first followed by a discussion of the predicted yields using information from short-time MD simulations. We then discuss the level of agreement and disagreement between the two sets of values and the ability to extrapolate the yield trends to different materials.

Experimental Information. In order to determine the number of sputtered water molecule equivalents per primary ion bombardment event, that is the total sputtering yield, depth profiles are measured for the H_3O^+ (m/z 19) ion and silver substrate Ag^+ (m/z 107) ion signal intensities from sequential mass spectra as a function of primary ion current and irradiation time (Figure 2). A typical depth profile plot of an ice film is characterized by three distinct regions: an initial increase in H_3O^+ intensity, an extended H_3O^+ sputter state, and the disappearance of the H_3O^+ intensity and appearance of Ag^+ intensity at the water ice/silver interface. The Ag^+ intensity decreases at the interface due to the presence of well-known matrix ionization effects and the fact that ion yields from clean metals tend toward zero.[22] The resulting profile can be used to assign the water ice/silver substrate interface region at the 50% maximum of 107 Ag^+ intensity and to determine the total amount of incident projectiles (N_p) required to erode the original 100−150-nm-hick water ice film. The quantity of water molecule equivalents removed during the profile (N_{H_2O}) was calculated using the known water ice film thickness, the irradiated sample area, and the water ice film molecular density (3.075×10^{22} molecules/cm^3). Accordingly, the average number of sputtered water molecules for each primary ion impact event ($Y_{H_2O/Projectile}$) can be easily determined using the relationship $Y_{H_2O/Projectile} = N_{H_2O}/N_p$. Depth profile experiments and consequent sputter yield calculations for each incident projectile were performed, and the Y_{H_2O} results are presented in Figure 3. The error bars are estimated to be approximately ±10%.

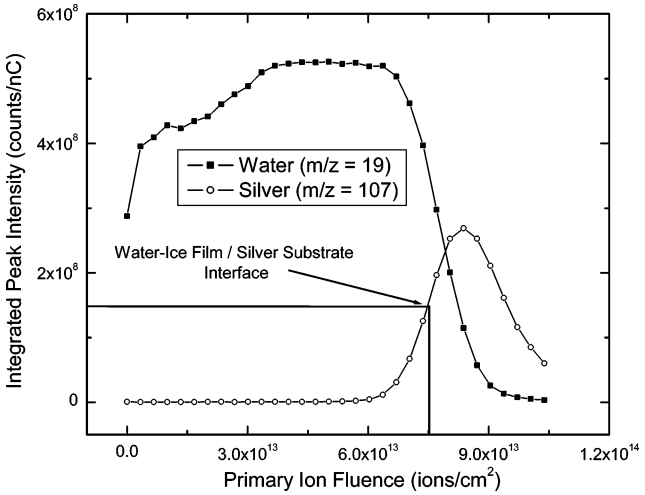

Figure 2. The 40-keV C_{60} depth profile through a 150-nm water ice film on a silver substrate. The bar lines represent the 50% maximum of $^{107}Ag^+$ intensity where the ice/silver interface was assigned. The depth profile plot indicates 4.0×10^{10} C_{60}^+ ions (7.5×10^{13} C_{60}^+/cm^2 fluence, 0.023 cm × 0.023 cm irradiation area) were required to remove 1.6×10^{14} water ice molecules (1×10^{-5} cm ice layer, 0.023 cm × 0.023 cm irradiation area, 3.075×10^{22} molecules/cm^3 density) from the water ice film. The profile measures ~4000 water molecule equivalents sputtered per incident 40-keV C_{60} impact.

The total sputtering yields for both C_{60} and Au_3 ion bombardment are several thousand water molecule equivalents per incident ion. For C_{60} bombardment, the yield varies almost linearly from 820 water molecule equivalents at an incident energy of 10 keV to 10 100 water molecule equivalents at 120 keV. For Au_3 bombardment, the yield varies almost linearly from 630 water molecule equivalents at an incident energy of 10 keV to 1200 water molecule equivalents at 25 keV. The values for 20 keV have been reported earlier[17] and are over 20 times larger than the yield for atomic Au bombardment at the same energy. Comparatively, the sputter yields for both Au_3 and C_{60} increase linearly as the primary projectile incident energy increases. The relative yield increase for Au_3 is smaller, however, than the relative yield increase for

(21) Russo, M. F.; Wojciechowski, I. A.; Garrison, B. J. *Appl. Surf. Sci.* **2006**, *252*, 6423−6425.

(22) Meyer, S.; Staudt, C.; Wucher, A. *Appl. Surf. Sci.* **2003**, *203*, 48−51.

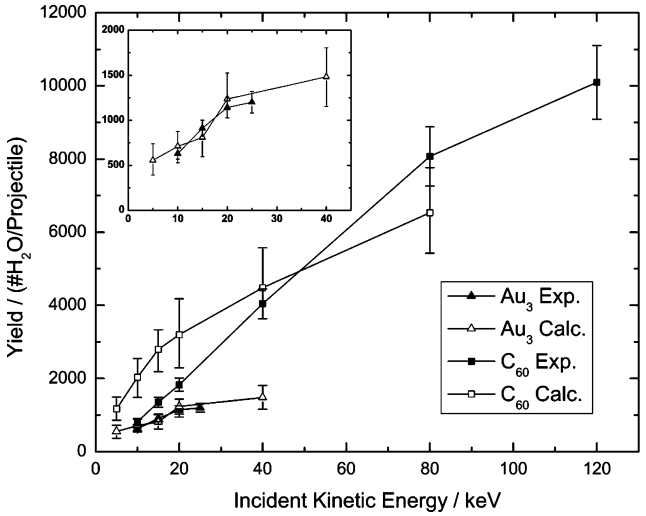

Figure 3. Measured and predicted total sputtering yields as a function of incident KE. The error bars are calculated using values of R_{cyl} ±3 Å from the estimated value. The experimental error bars are approximated ±10%. The inset highlights the Au_3 experimental and calculated data.

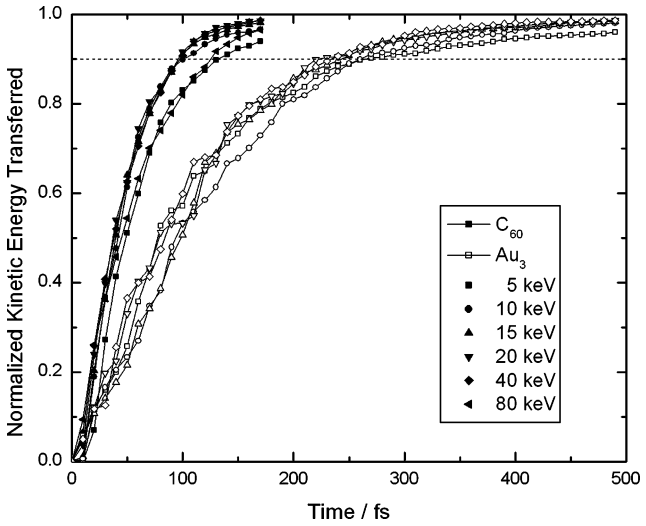

Figure 4. Energy transferred to the substrate for C_{60} and Au_3 bombardment at energies between 5 and 80 keV. The energies are normalized to the incident energy.

C_{60} over equal increases in primary ion kinetic energy. Moreover, the linear trend for the increase in yield changes between 20 and 40 keV for Au_3 and somewhere between 80 and 120 keV for C_{60}. Discussion involving the variations in Au_3 and C_{60} sputter yield trends and its significance to molecular dynamic simulations will be presented later in this section.

Computational Information. The first step in applying the MEDF model is to determine the time at which 90% of the cluster energy has been transferred to the substrate. The energy transferred versus time for each of the systems is illustrated in Figure 4. The transfer rate is relatively independent of energy for each cluster, with all C_{60} bombardment events requiring ~100 fs and all Au_3 bombardment events requiring ~250 fs to reach 90% energy transfer. Representative contour plots of the excitation track at 90% energy transfer times for 10-, 20-, and 40-keV bombardment are shown in Figure 5 along with lines to illustrate the R_{cyl} estimates. As discussed in our previous paper, the vertical component of energy is not included in the plots in order to make the comparison with the track model more consistent.[18] These plots represent the average excitation energies within concentric rings of the substrate originating along the axis of impact. This method is used in order to obtain a more defined boundary between the excitation track and bulk of the substrate by removing direction-specific anomalies that occur when taking a slice down the middle of the sample as was done previously.[18]

Estimates of the cylinder radii have been made based upon the information from the plots in Figure 5 along with those for the other incident energies not shown. The physics dominating the energy flow appear to be primarily dependent upon the repulsive interactions among the water ice molecules. This conclusion has been drawn from the remarkably similar values of R_{cyl} for C_{60} and Au_3, which show only a minimal increase with increasing incident energy.

The average excitation energy $\tilde{E}$ for each system is calculated from the determination of R_{cyl} and is given in Figure 6. The excitation energy in the surface region for Au_3 is relatively constant with respect to incident KE because the energy is deposited deep into the sample as illustrated by the contour plots of Figure 5. For C_{60} bombardment, however, most of the energy transferred is localized in the near-surface region and there is a substantial increase in excitation energy with increasing KE. When the energy associated with the vertical component of motion is removed from the substrate molecules in this analysis, it is evident that the distribution of energy transferred to the substrate is becoming increasingly more dependent on the directionality of the C_{60} cluster; the energy track is increasingly more cylindrical. As the incident energy is increased to 40 keV and above, there is a leveling off of the excitation energy due to a more elongated cylindrical deposition similar to that of Au_3.

The predicted yields from the MEDF model using the values of R_{cyl} and $\tilde{E}$ of Figure 6 are shown along with the experimental data in Figure 3. Of note is that there are no adjustable parameters in our model and the values are plotted on a linear scale. The error bars on the predicted yields correspond to calculating $\tilde{E}$ for values of R_{cyl} that are ±3 Å from the determined value. The agreement between the calculated and measured yields for Au_3 bombardment is within experimental error whereas the predicted C_{60} yields are about a factor of 2 larger.

The yield of water ice sputtered due to Au_3 bombardment exhibits a slow increase with increasing KE. The main effect of the increase is the increasing value of R_{cyl} upon which the total yield has a cubic dependence. The MD simulations clearly show that the Au_3 is depositing its energy deep in the system, and the MEDF model explains that it is implanted too deep in the sample to maximize its effectiveness for ejecting material. Previous simulations for 5-keV bombardment indicate that the Au_3 particles would be implanted in the substrate,[21] a prediction observed in experiment. As the energy of the Au_3 increases, the implantation only gets deeper. The two main reasons that the Au atoms implant are the relatively large initial KE and the heavy mass of the Au atom relative to the water ice molecule. Because these conditions will be the same for all organic substrates, a similar trend of yield with increasing KE as shown in Figure 3 is expected to be valid for many organic and biological molecular solids.

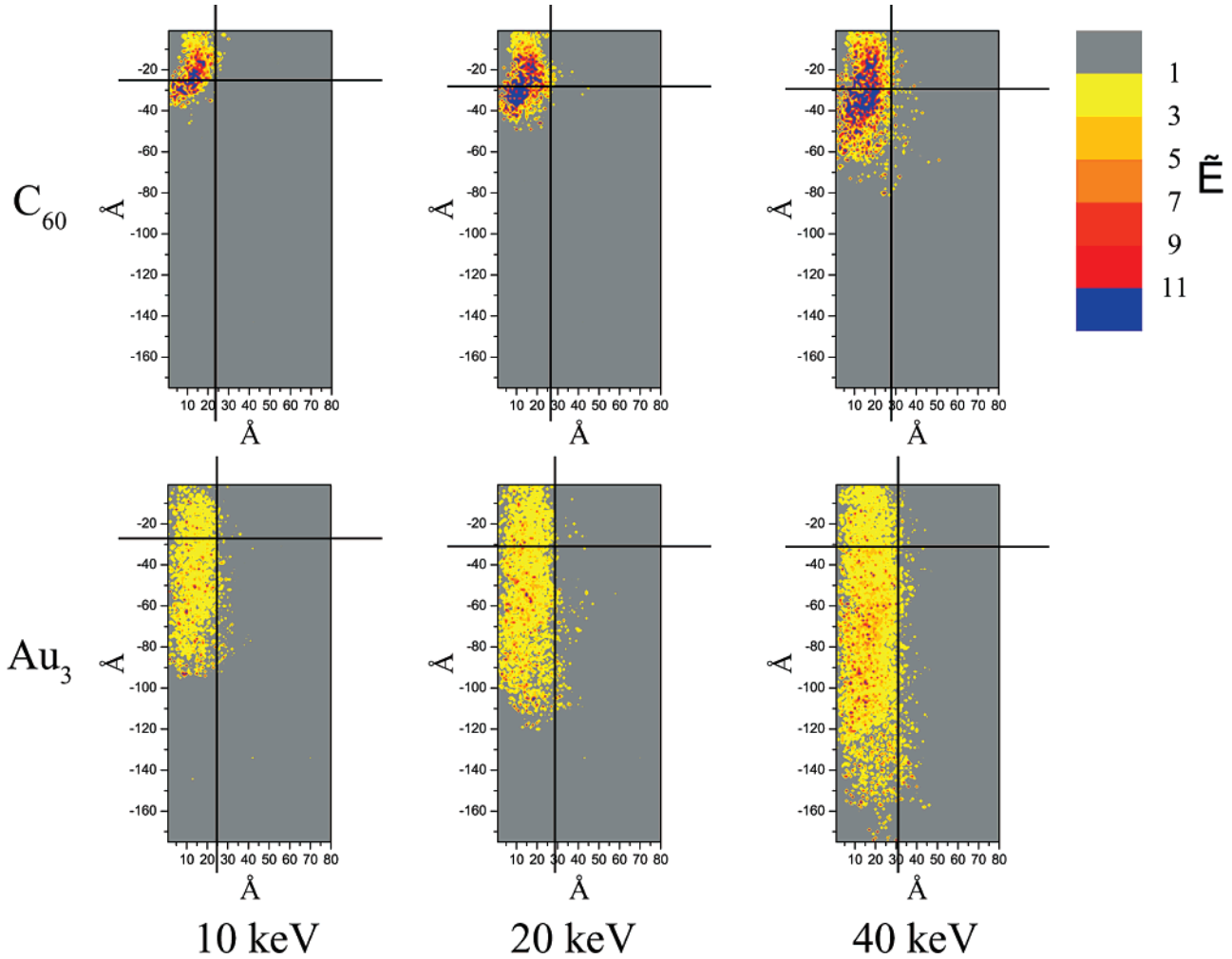

Figure 5. Contour plots of the excitation energy $\tilde{E}$ for C_{60} and Au_3 bombardment at energies 10, 20, and 40 keV. There is an implied cylindrical symmetry around the left edge of the figures. The black lines represent the position of R_{cyl}.

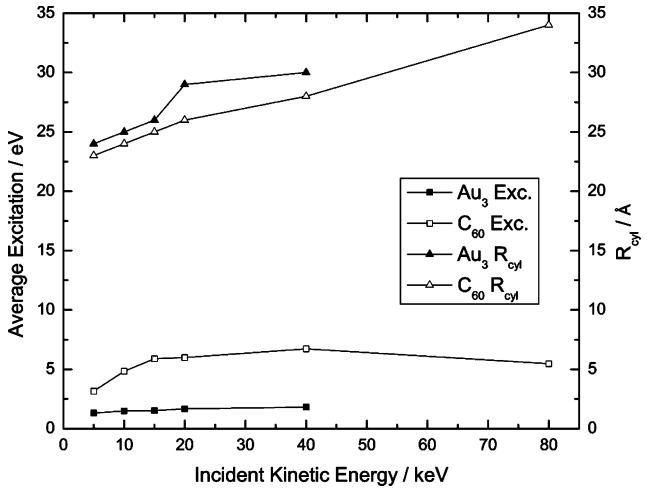

Figure 6. Values of R_{cyl} and $\tilde{E}$ as a function of incident KE. The error bars on the values of R_{cyl} are ±3 Å.

The yield of water ice sputtered due to C_{60} bombardment increases with increasing KE as the incident energy is deposited in the near-surface region and can effectively contribute to the ejection processes. The increase in yield with increasing KE is due mainly to the increasing value of $\tilde{E}$ rather than changes in R_{cyl}. In simulations of C_{60} bombardment on a coarse-grained representation of solid benzene, it was also found that the C_{60} deposits its energy in the same depth independent of incident KE;[23] thus, we believe this trend of increasing yield in increasing KE to be valid for many molecular solids.

The agreement between the calculated and experimental yields for C_{60} bombardment is outside the estimated error bars. In addition, some aspects of the trend for the experimental and calculated C_{60} yields as a function of KE are different. There are several possible reasons for the discrepancies. First, the agreement in predicted yield from the MEDF model and the MD simulations for 5-keV bombardment is not perfect.[18] In particular, the atoms do not eject exactly from the conical region as shown in Figure 5 of ref 16. Second, the deposition of energy due to C_{60} bombardment is more spherical rather than cylindrical as shown in Figure 4, especially for 20 keV and below. It is unknown how material would flow from a spherical region. It is possible that the assumption of a cylindrical track is overestimating the yield at energies below 20 keV and is less of an approximation above 20 keV. Third, the description of water ice is as a rigid molecule with no dissociation, reaction, or electronic events taken into account. Simulations of C_{60} and Au_3 bombardment on water ice

(23) Smiley, E. J.; Winograd, N.; Garrison, B. J. *Anal. Chem.* **2007**, *79*, 494–499.

using a potential that allows for bond dissociation into ions demonstrates that there are many reactions in the near-surface region for C_{60} bombardment whereas for Au_3 bombardment the dissociation events are spread throughout the motion of the Au atoms.[24] If significant energy is flowing into a reaction or electronic channel, then there would be less energy available for ejection processes and the predicted yield would be too high. Moreover, since the energy deposition at the lower incident energies is more confined to the surface region, the error would be greatest at the lower energies. Finally, the simulations were performed for a perpendicular angle of incidence because the concept of having a cylindrical track would break down for off-normal angles. The experiments, on the other hand, were performed for an angle of incidence of 40°.

The MEDF model allows us to now qualitatively understand the previously reported sputtering yields of water ice due to 20-keV Au^+ and Au_2^+ bombardment.[16,17] This explanation is performed with the caveat that the atomic and diatomic bombardment events probably do not create as definitive a track as the cluster bombardment. Simply because the energy per particle changes from 20 to 10 to 6.67 keV for Au, Au_2, and Au_3, respectively, we would expect the depth of energy deposition to be largest for Au and the energy deposited near the surface to be the least. Thus, the water ice sputtering yield due to Au bombardment is the smallest, followed by Au_2 and Au_3.[16]

There are several possible implications from these calculations for imaging and depth profiling that are important. For Au_3 bombardment, the total sputtering yield increases as the KE increases from 10 to 25 keV and thus higher KE should increase the ion signal. The values of R_{cyl} and R_s are on the order of 30 Å and are smaller than the current beam size of 1000 Å.[25] Although Figure 5 does not show the final positions of the Au atoms, it is clear that, as the KE of the Au_3 ion increases, the depth of deposition of the Au atoms increases and also the potential for chemical reactions increases.[24] For C_{60} bombardment, the yield increases with increasing KE, thus also potentially increasing the ion signal. For energies below 20 keV, the energy is deposited in approximately the same depth as the volume of ejected material. For higher KE, the deposited energy is deeper; thus, there is the potential for more damage to be left in the substrate. Whether the enhancement of yield will offset the additional damage has yet to be determined by experiment. The values of R_s for C_{60} can be up to 80 Å for the largest KE, but this value is insignificant compared to the beam size of several hundred nanometers. As argued above, we believe these conclusions to be applicable to other organic molecular solids.

(24) Ryan, K. E.; Wojciechowski, I. A.; Garrison, B. J. *J. Phys. Chem. C* Submitted.
(25) Jones, E. A.; Lockyer, N. P.; Vickerman, J. C. *Int. J. Mass. Spectrom.* **2007**, *260*, 146−157.

CONCLUSIONS

Experimentally measured total sputtering yields for water ice as a function of incident kinetic energy for C_{60} and Au_3 ion bombardment have been presented. Using the mesoscale energy deposition footprint model and short-time molecular dynamics simulations, we have predicted the yields with no adjustable parameters. For Au_3 bombardment, we find that the initial kinetic energy is deposited too deep in the sample to make effective use of the energy for ejection. As the primary ion energy increases, more energy is wasted relative to energy deposited in the near-surface region; thus, the yield increase in incident KE is small. For C_{60} bombardment, however, the energy is effectively deposited in the near-surface region and the yield increases more dramatically with increasing cluster KE.

ACKNOWLEDGMENT

The authors thank the Chemistry Division of the National Science Foundation for their support of the computational research (CHE-0456514), the NIH (EB002016-13) for providing funds to construct the C_{60} source, and the NSF (CHE-0555314) and DOE (DE-FG02-06ER15803) for providing graduate student support. We also acknowledge Zbigniew Postawa, Kate Ryan, and Ed Smiley for their insight and helpful discussions.

Received for review January 17, 2007. Accepted April 13, 2007.

AC070105L